Assessment of the Risk of Blastomere Biopsy during Preimplantation Genetic Diagnosis in a Mouse Model: Reducing Female Ovary Function with an Increase in Age by Proteomics Method

Yang Yu,[†,‡,§,#] Yue Zhao,[†,§,#] Rong Li,[†,§,#] Li Li,[†] Hongcui Zhao,[†] Min Li,[†] Jiahao Sha,[||] Qi Zhou,[⊥] and Jie Qiao*[,†,‡,§]

[†]Center of Reproductive Medicine, Department of Obstetrics and Gynecology, Peking University Third Hospital, No. 49 HuaYuan Bei Road, HaiDian District, Beijing 100191, China

[‡]Beijing Key Laboratory of Reproductive Endocrinology and Assisted Reproductive Technology, No. 49 HuaYuan Bei Road, HaiDian District, Beijing 100191, China

[§]Key Laboratory of Assisted Reproduction, Ministry of Education, No. 49 HuaYuan Bei Road, HaiDian District, Beijing 100191, China

[||]Laboratory of Reproductive Medicine, Department of Histology and Embryology, Nanjing Medical University, No. 140 Hanzhong Road, Gulou District, Nanjing 210029, China

[⊥]State Key Laboratory of Reproductive Biology, Institute of Zoology, Chinese Academy of Sciences, No. 1 Beichen Xi Road, Chaoyang District, Beijing 100101, China

S *Supporting Information*
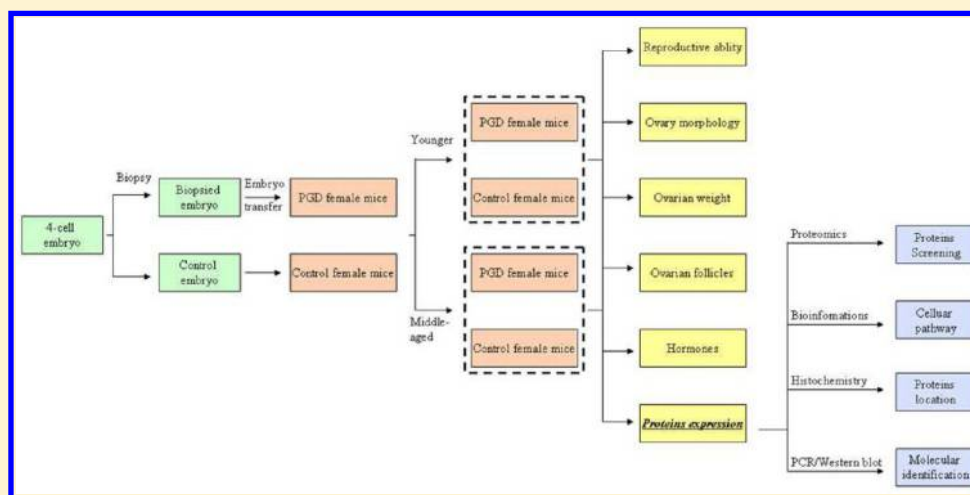
ABSTRACT: Preimplantation genetic diagnosis (PGD) is important for screening genetic and chromosome mutations in embryos so that the efficiency of assisted reproductive treatment can be increased and birth defects can be decreased; however, some studies have reported a risk from this technology as well as other assisted reproductive technologies. We have developed a blastomere biopsy mouse model to assess the potential effects of blastomere biopsy that was one key procedure in PGD on the fertility of female mice at different ages. We showed that female fertility was decreased in the biopsied mouse model with an increase in age. Moreover, the ovarian weight, serum hormone levels, and the number of primordial, primary, preantral, and antral stage follicles were also decreased in the middle-aged biopsied mouse model. To elucidate the underlying molecular mechanism, we did proteomics analysis on ovarian tissues from puberty biopsied and nonbiopsied mice of the 23 differentially expressed proteins that were screened for in both groups, 3 proteins (PSMB8, ALDH1A1, and HSPA4) were selected and identified by Western blotting and quantitative RT-PCR methods, which showed the 3 proteins to regulate 12 cellular pathways. Furthermore, these three proteins were shown to be located in ovarian tissues, and the dynamic changes of expression profiling in middle-aged biopsied and nonbiopsied mice were demonstrated. The present study showed that blastomere biopsy technology impairs fertility when mice are middle-aged, which possibly resulted in abnormal expression profiling of PSMB8, ALDH1A1, and HSPA4 proteins. Thus, additional studies should be performed to assess the overall risk of blastomere biopsies during PGD procedures.

KEYWORDS: *preimplantation diagnosis, embryo biopsy, ovary function, female fertility, proteomics*

INTRODUCTION

Assisted reproductive technology (ART) has been widely used worldwide since the first "test tube baby" was born in the United Kingdom in 1978.[1] Traditional ART was developed to facilitate pregnancies in couples with reproductive system diseases; however, with the advent of preimplantation genetic diagnosis (PGD) in 1990,[2] infertile couples experiencing recurrent miscarriage or X-chromosome-linked diseases are most likely to benefit from it. Indeed, PGD has gained widespread application not only in X-linked genetic diseases and chromosome aneuploidy analysis but also in single gene disorders by array comparative genomic hybridization (aCGH) and single nucleotide polymorphism (SNP)-based arrays.

The PGD procedure includes two key parts, as follows: genetic detection using a molecular method that has been developed recently to detect more genetic mutations, including uniparental disomy, parental origin of aneuploidies, genetic parentage, and unbalanced translocations in all chromosomes, and embryo biopsy in the eight-cell or blastocyst stage, or polar body biopsy, in which an eight-cell biopsy is currently the most widely used in clinics.[3,4] Because fertilized embryos are biopsied using additional micromanipulation, the effects of the biopsy procedure used in PGD on embryo development in pre- and postimplantation stages is disconcerting to many researchers.

On the basis of classic developmental biology dogma, the blastomere in the early developmental stage is totipotent and has the ability to develop into an individual. On the basis of this notion, embryo splitting at two-cell stage has been used in animal models, including mice,[5] rabbits,[6] sheep,[7] bovine,[8] goat,[9] and horse,[10] and in a preliminary nonhuman primate study involving one rhesus monkey[11] without obvious effects of embryo micromanipulation on artificial twins, although the efficiency of embryo development was arguable. Blastomere from eight-cell embryo could contribute to the viable animal by nuclear transfer or quimeras technology, however, there were no reports about the birth of animals using blastomere from eight-cell embryos when this single blastomere was incubated in vitro and transferred into the recipient. Moreover Fleming observed cell-surface polarity in mouse eight-cell blastomeres,[12] and this was also proved by Levy et al.[13] The location of the surplus blastomeres would be rearranged if one blastomere was removed, which resulted in the changes of cell interactions, ion exchanges, and chemical agents distribution in the blastomere; therefore, the development of embryos would be impaired. Of importance, the risk of embryo micromanipulation has been studied and evaluated using mouse models in some studies, including in vitro fertilization (IVF) and intracytoplasmic sperm injection (ICSI), and a retrospective analysis of the clinic setting has suggested a potential risk with IVF and ICSI.[14,15] PGD has been available in the last 10 years, although the first clinical case was reported in 1990,[2] and the number of offspring conceived using this technology has not been compared with IVF or ICSI and the majority of children are ~10 years of age. Thus, it is difficult to evaluate the risk of PGD based on a follow-up survey, although Desmyttere et al. recently indicated that embryo biopsy for PGD did not introduce extra risk to the overall medical condition of 995 newborn children compared with ICSI between 1993 and 2008.[16] In 2009, we first evaluated the effects of embryo biopsy on offspring behavior and physiology and demonstrated the potential high risk for neurodegenerative disorders by proteomics analysis, which suggested that blastomere biopsies during the PGD procedure require further study and evaluation.[17]

In recent years, some studies have focused on the effects of ART on the reproductive system of male offspring in human clinics or animal models. Feng et al. reported that the incidence of de novo Y chromosome microdeletion in male children conceived through ICSI or IVF was statistically higher than that in those conceived naturally,[18] and Yu et al. also reported that ICSI induces the apoptosis of spermatocytes in testes in ICSI mouse models;[19] however, no comparable study involving the female reproductive system has been conducted.

In the present study, we mainly focused on the effects of blastomere biopsy on the ovaries of puberty and middle-aged mouse models conceived from PGD and investigated the protein expression profiles in puberty ovaries. Our results indicate that microinjection manipulation used in ICSI might pose potential risks to ovarian tumors of female mice.

MATERIALS AND METHODS

The chemical agents for serum hormone measurement were purchased from Roche company, and the antibodies for protein identification were purchased from Abcam company, and the other chemicals were obtained from Sigma Chemical (St. Louis, MO). The study was approved by the Institutional Review Board of Peking University Third Hospital.

Mouse

The mice used in this study were housed and bred in the Animal Center of the Medical College of Peking University according to the national legislation for animal care. All mice were maintained under controlled temperature and lighting conditions and given food and water ad libitum. There are corn, beans, fish flour, flour, bran, salt, calcium bicarbonate, vitamins (A, D, E, K, B1, B2, B6, B12, etc.), microelements (Na, K, Mg, Cu, Fe, Zn, Mn, I, Se, Ca, P, etc.), and essential and nonessential amino acids in mouse feed.

Construction of Mouse Model by Embryo Biopsy

Zygotes were collected from the fallopian tubes of superovulated adult female mice (8−12 week-age) in the 20 h after mating with adult male mice (8−12 weeks of age). On the second day, the four-cell embryos were partially biopsied, and one blastomere was removed from the zona pellucida by a beveled glass pipet with an inner diameter of 15−18 μm, which was designed as the biopsied group. The other four-cell embryos served as control groups and were designed as the nonbiopsied group. The reconstructed "three-cell" and control four-cell embryos were immediately transferred into the fallopian tubes of pseudopregnant female mice, and the mice in the biopsied and nonbiopsied groups were delivered naturally on day 19.5 of gestation. Ten-week-old mice were considered to puberty, and 40-week-old mice were considered to be middle-aged.

Fertility Assay

Ten female mice in the biopsied and nonbiopsied groups were mated with male mice, and the vaginal plug was checked the next morning. The female mice with a plug were housed and bred separately, and the pregnant mice were delivered naturally on day 19.5 of gestation. The efficiency of plug and pregnancy as well as the litter size and ratio of male-to-female neonates were recorded.

Histologic and Histomorphometric Analyses of Ovarian Tissues

Puberty (10 week old) and middle-aged mice (40 week old) in both groups were sacrificed, and the ovarian tissues were collected. The ovaries were weighed before fixation. Histologic and

histomorphometric analyses were conducted according to the previous study.[20] Ovaries from puberty and middle-aged ART mice were fixed in bouin solution and embedded in paraffin. After deparaffinizing sections, the section slides were rehydrated in steps with distilled water (dH$_2$O); then, the sections of ovaries were stained with hematoxylin and eosin (HE) for histologic examination.

Enumeration of Follicles

The number of follicles from five sequential ovarian tissue sections in each mouse was calculated. Following the classification criterion described in the previous study,[21] the follicles were divided into four parts (primordial, primary, preantral, and antral follicles). The number of follicles was also recorded and analyzed in biopsied and nonbiopsied mice.

Measurement of Steroids

Mouse blood was collected from the retro-orbital sinus. First, the eyeball was quickly removed from the socket with a pair of tissue forceps. Then, blood was collected into a tube with coagulant accelerant that mainly contained silicon dioxide and lectin, and the serum was collected after centrifugation at 300g at 4 °C. The estradiol (E2), progesterone (PRG), testosterone (T), and androstenedione (AND) levels were determined using chemiluminescence with an Immunoassay System (Roche). The sample was mixed with the corresponding biotinylated antibody, derivative labeled with Ru, and Danazol, and the hormone in the sample would compete the binding site with their derivative. After adding particle packaged by streptavidin, the immunocomplex would bind onto this particle by the reaction between biotin and streptavidin. Finally, the mixture was transferred into the testing pool, and the particle would be adsorbed onto the electrode, and the sample was tested by chemiluminescence after voltage was enhanced. The data were analyzed by comparing with standard curve

Estrous Cycle Examination

The estrous cycles of puberty and middle-aged female mice in each group were tested using a vaginal cytology method, as previously described.[22] Ten female mice in each group were examined daily, and the estrous cycle was determined using a vaginal smear flushed with physiologic saline and identified under a microscope. Methylene blue staining was performed to identify the vaginal epithelial cells. The days of the estrous cycles were recorded over 10 days.

Proteomics Experiment

Reagents. Urea, 3-[(3-cholamidopropyl)-dimethylammonio]-1-propane sulfonate (CHAPS), immobilized pH gradient strips (IPG strips), immobilized pH gradient buffer (IPG buffer), Tris, molecular weight markers, acrylamide, diacrylamide, SDS, ammonium persulphate (APS), N,N,N',N'-tetramethylethylenediamine (TEMED), iodoacetamide, and glycerol were from GE Healthcare (Uppsala, Sweden). Thiourea, acetonitrile (ACN), ammonium bicarbonate (NH$_4$HCO$_3$), trifluoracetic acid (TFA), formaldehyde, and matrix material (α-cyano-4-hydroxy cinnamic acid, α-HCCA) were from Sigma Chemical (St. Louis, MO). HaltTM protease inhibitor cocktail and EDTA-free were from PIERCE (Rockford, IL). Sequencing-grade-modified trypsin (trypsin) was obtained from Promega (Madison, WI). Peptide calibration standards were purchased from Bruker (Bruker Daltonik, Bremen, Germany). Dithiothreitol (DTT) was from Shenggong (Shanghai, China).

Sample Preparation. Brain specimen was collected from each experimental animal and divided immediately on ice into two parts, which were either fixed in 4% polyformaldehyde solution for histological examination or snap-frozen in liquid nitrogen for protein isolation. Protein lysates were isolated after crushing the tissues in liquid nitrogen with a mortar and then were extracted with lysis buffer containing 7 M urea, 2 M thiourea, 4% (w/v) CHAPS, 65 mM DTT, 2% (v/v) IPG buffer pH 3−10, NL, and 1% (v/v) inhibitor protease cocktail. The extracts were centrifuged at 40 000g for 1 h, and the supernatants were stored at −70 °C. The concentrations of extracts were determined by the method of Bradford.[23]

Two-Dimensional Gel Electrophoresis. Isoelectric focusing (IEF) was carried out using commercially available, dedicated apparatus: IPGphor (GE Healthcare, Uppsala, Sweden). IPG strips, nonlinear pH 3−10, 24 cm long were used. Samples containing 80 μg protein were rehydrated and focused at 20 °C, as previously described.[24] After IEF, the IPG strips were equilibrated, then run in Ettan-Dalt six electrophoresis system (GE Healthcare, Uppsala, Sweden) and visualized by silver staining according to the published procedure, except that glutardialdehyde was omitted in the sensitizing solution.[25]

Protein Spot Detection and Statistical Analysis. Two-dimensional electrophoresis of each sample was performed. The gels were scanned in Atrix scan 1010 plus (Microtek, Taiwan, China), and resulting images were analyzed using the Image-MasterTM 2D Platinum software (GE Healthcare, Uppsala, Sweden) for spot detection, quantification, and comparative and statistical analyses. The amount of protein present in each spot was given as its volume, which was calculated as the volume above the spot border, situated at 75% of the spot intensity, as measured from the peak of the spot. To exclude variations due to protein loading and staining, we used relative volume (% vol), which normalized the spot volume as a percentage of the total volume of all of the spots present in a gel; this normalization allowed protein expression differences to be evaluated between gels. The spot volumes from each experimental groups were pooled, respectively, for the calculation of the mean ± standard error of the mean (SEM), and an independent t test was performed to determine the significant differences between the groups. P values <0.05 were considered to be statistically significant.

In-Gel Tryptic Digestion. Detected spots were excised, washed with 100 μL of water thrice, dehydrated in ACN, and dried at room temperature. The gel pieces were reduced with 10 mM DTT/25 mM NH$_4$HCO$_3$ at 56 °C for 1 h, alkylated with 55 mM iodoacetamide/25 mM NH$_4$HCO$_3$ for 45 min at room temperature in darkness, washed with 25 mM NH$_4$HCO$_3$, and then dehydrated with 50% ACN and 100% ACN in seccession. The dried gel pieces were reswollen with 2 to 3 μL of trypsin solution (trypsin at a concentration of 10 ng/μL in 25 mM ammonium bicarbonate); after they were incubated at 4 °C for 30 min, excess liquid was discarded and gel plugs were incubated at 37 °C for 12 h. Then, TFA was added until the final concentration was 0.1% to stop the digestive reaction.

MALDI-TOF MS Analysis. Digests were immediately spotted onto 400 μm anchorchip (Bruker, Germany). Spotting was achieved by pipetting 1 μL of analyte sample onto the MALDI target plate twice and then adding 0.05 μL of 2 mg/mL α-HCCA in 0.1% TFA/33% ACN that contained 2 mM ammonium phosphate. Bruker peptide calibration mixture was spotted down for external calibration. All samples were allowed to air-dry at room temperature, and 0.1% TFA was used for on-target washing. The samples were analyzed in a time-of-flight Bruker Biflex IV mass spectrometer (Bruker, Germany). The spectrometer was run in positive ion mode and in reflector mode

with the accelerating voltage of 19 kV. The annotations of the peak masses in the spectrum that were generated by the felxAnalysis processing software (Bruker, Germany) were checked and edited manually to ensure the correct peaks were labeled, and to remove the masses that arose from the matrix, trypsin, or known contaminants (e.g., keratins). The edited peak lists were used for database searches with search program MASCOT (http://www.matrixscience.com/). The following search parameters were applied: SWISS-PROT and TrEMBL were used as protein sequence databases; a mass tolerance of 100 ppm and one miss cleavage were allowed, alkylation of cysteine by carbamidomethylation was considered as fixed modification and oxidation of methionine was considered as variable modification; five matching peptides were the minimal requirement for an identity assignment. The peptide masses were compared with the theoretical peptide masses of all available proteins from *Mus musculus*. The algorithm used for determining the probability of a false positive match with a given MS spectrum is described elsewhere.[26]

Pathway Analysis by PathwayStudioTM

The cellular process, possibly influenced by the differentiated proteins in both groups, was performed with PathwayStudioTM software (version 5.0; Ariadne Genomics, Rockville, MA). In our analysis, the identified cellular processes were all confirmed manually using PubMed/Medline hyperlinked abstracts. The first four genes that were involved in most cellular pathways were screened, including VCL, HSPA4, ALDH1A1, and PSMB8.

Real-Time Quantitative Polymerase Chain Reaction

To verify the differentially expressed proteins screened from proteomics analysis, we found the corresponding genes in the NCBI/PubMed database. Five ovarian samples per group were subjected to real-time PCR using the following primers: GAPDH, VCL, HSPA4, ALDH1A1, and PSMB8 (Supplemental Table 1 in the Supporting Information). The melting (dissociation) curves of the PCR reactions were monitored to ensure a single PCR product and no primer dimer. All experiments were repeated 40 cycles. The real-time PCR results were analyzed using ABI Prism 7000 SDS software (Applied Biosystems, Foster City, CA).

Western Blotting

The proteins from five ovarian samples in each group were extracted and transferred to polyvinylidene fluoride membranes that were blocked in Tris-buffered saline solution with 0.1% Tween 20 and 5% skim milk for 2 h. Then, the blots were incubated with the primary antibody overnight at 4 °C, including anti-HSPA (1:200; Abcam), anti-VCL (1:200; Abcam), anti-ALDH1A1 (1:200; Abcam), and anti-PSMB8 rabbit polyclonal antibodies (1:200; Abcam). After washing three times in Tris-buffered saline solution with 0.1% Tween 20, the membranes were incubated for 1 h at 37 °C, with 1:2000 horseradish peroxidase-conjugated appropriate secondary antibodies. Finally, the membranes were processed and visualized using an enhanced chemiluminescence detection system (Amersham Pharmacia Biotechnology, Piscataway, NJ).

We estimated the relative amount of the target proteins using a housekeeping protein as internal control (*β*-actin). We determined the intensity of bands by Carestream MI software (Kodak) and performed the quantitative analyses of each gray numerical value of target protein versus that of individual *β*-actin. The average values were calculated from three individual control samples or four individual PGD samples and presented as mean ± SD, and statistical differences compared with controls were illustrated as *,$P < 0.01$.

Immunohistochemistry Staining

One part of the ovarian sections was deparaffinized, then the slides were rehydrated in steps with dH_2O and immersed in 0.5% v/v hydrogen peroxide/methanol for 10 min. The slides were incubated with the primary antibody overnight at 4 °C in a humidified chamber, then reacted with the secondary antibody for 30 min. Diaminobenzidine was used as a chromogen, and the sections were counterstained with hematoxylin. The primary antibody was omitted to create negative controls.

Statistical Analysis

The fertility assay, ovarian weight, follicle number, hormone levels, estrous cycle days, and RT-PCR data were analyzed using a *t* test for significant differences between the two groups. A $P < 0.05$ was regarded as a significant difference.

■ RESULTS

To assess the fertility capacity of female biopsied mice, 10 mice in each group were mated with 10- and 40-week-old fertile male mice. In the puberty mice, all females had vaginal plugs in the days following mating with male mice and became pregnancy regardless of group (Biopsied or nonbiopsied), and there were also no significant differences in litter size and the number of male and female pups ($P > 0.05$; Figure 1A). In the middle-aged group, no mice became pregnant in the biopsied group, although there were two mice with vaginal plugs after mating, but the number of mice with vaginal plugs and resulting pregnancies in the nonbiopsied group was significantly higher than those in the biopsied group ($P < 0.05$). Accordingly, the litter size and the number of male and female pups were also increased compared with the biopsied group ($P < 0.05$; Figure 1B). Regardless of the differences in age of the biopsied and nonbiopsied mice in the puberty and middle-aged groups, the offspring were delivered by natural labor, and the birth weights and male-to-female birth ratio of the offspring were not significantly different ($P > 0.05$; Figure 1C).

Furthermore, the ovarian morphology and weight were assessed in puberty and middle-aged mice from the biopsied and nonbiopsied groups. The results indicated that there were no significant differences in ovarian weight in the puberty mice regardless of the biopsied or nonbiopsied models ($P > 0.05$); however, the ovarian weight in the biopsied group was decreased compared with the nonbiopsied group when the mice were middle-aged ($P < 0.05$; Figure 2A). The morphology of the ovaries was normal in each group (Figure 2B,C). Moreover, the follicles were calculated from the five sequential ovarian tissue sections by HE treatment in the biopsied and nonbiopsied groups, and the total number of follicles and follicles in the primordial, primary, preantral, and antral stages was calculated and compared between the biopsied and nonbiopsied groups. The results were similar with fertility assay experiments. In the puberty group, the total number of follicles and follicles in the four different stages was not significantly different in comparing the biopsied and IVEM groups ($P > 0.05$, Figure 3A). In the middle-aged group, the total number of follicles was significantly decreased in the biopsied group ($P < 0.05$), and the number of follicles in the preantral and antral stages was also significantly lower than the nonbiopsied group ($P < 0.05$). The number of follicles in the primordial and primary stages in the biopsied groups was not significantly different compared with the nonbiopsied group ($P > 0.05$; Figure 3B).
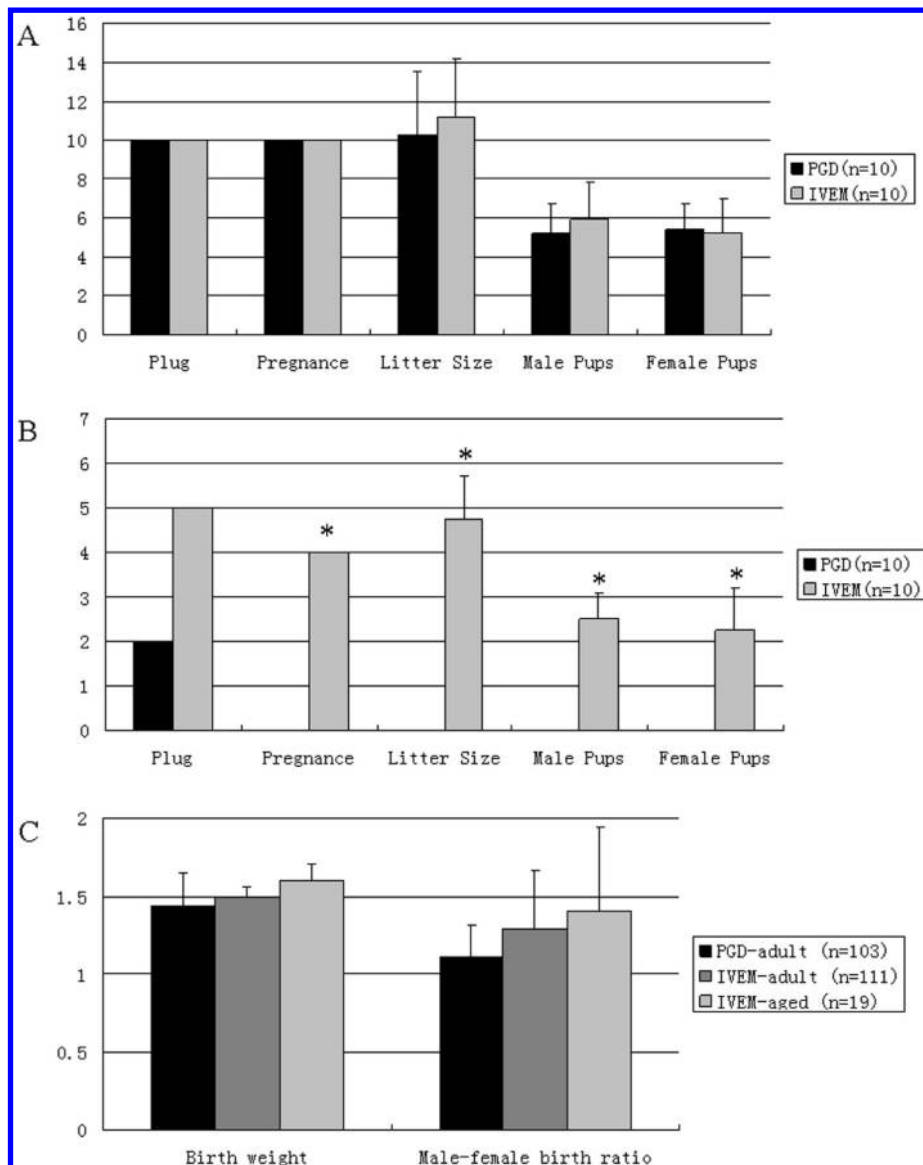
Figure 1. Fertility assay of mice in the biopsied and nonbiopsied groups at different ages. (A) Puberty 10-week-old mice. (B) 40-week-old middle-aged mice. * indicates a significant difference, $P < 0.05$.

Furthermore, histologic examination of the ovaries from puberty and middle-aged female mice in both groups was performed. The morphology of ovarian tissues from puberty mice, regardless of biopsied or nonbiopsied groups, appeared normal, and there were follicles in every developmental stage and the degenerated corpus lutea in the section samples (Figure 3C,D). In comparing middle-aged biopsied and nonbiopsied mice, some follicles in the growth stage in the nonbiopsied group could be observed at the cortex of ovarian, including preantral and antral follicles, and the atretic follicles were observed in the ovary. Preantral, antral, and atretic follicles were also observed in the ovary tissue sections collected from biopsied mice, although the number of preantral and antral follicles was significantly decreased compared with nonbiopsied mice as previously shown (Figure 3B,E,F).

The steroid levels were tested in the biopsied and nonbiopsied groups, including estradiol, progesterone, testosterone, and androstenedione. In agreement with previous experiments, no difference was found in both groups among the four steroid levels when the mice were puberal ($P > 0.05$). In the middle-aged

group, there were also no significant differences in the progesterone level ($P > 0.05$); however, the estradiol, testosterone, and androstenedione levels in the biopsied group were significantly lower compared with the IVM group ($P < 0.05$; Table 1).

For estrous cycle examination, there was no significant difference in the puberty biopsied and nonbiopsied groups (4.39 vs 4.23 days; $P > 0.05$); however, the diestrus days were significantly prolonged in the middle-aged biopsied mice, thus the days of the estrous cycle were also significantly longer than the middle-aged nonbiopsied group ($P < 0.05$; Table 1).

To investigate the possible molecular mechanisms underlying the induction of ovarian tissue abnormalities in the biopsied group, proteomics analysis was performed to screen the differentially expressed proteins. After 2-DE treatment, the gels from puberty biopsied and nonbiopsied ovarian tissues were individually imaged and analyzed using ImageMaster™ 2D platinum software (Figure 4A), and the detailed information to show the dots for some of differentially expressed proteins is shown in Supplementary Figure 1 in the Supporting Information.
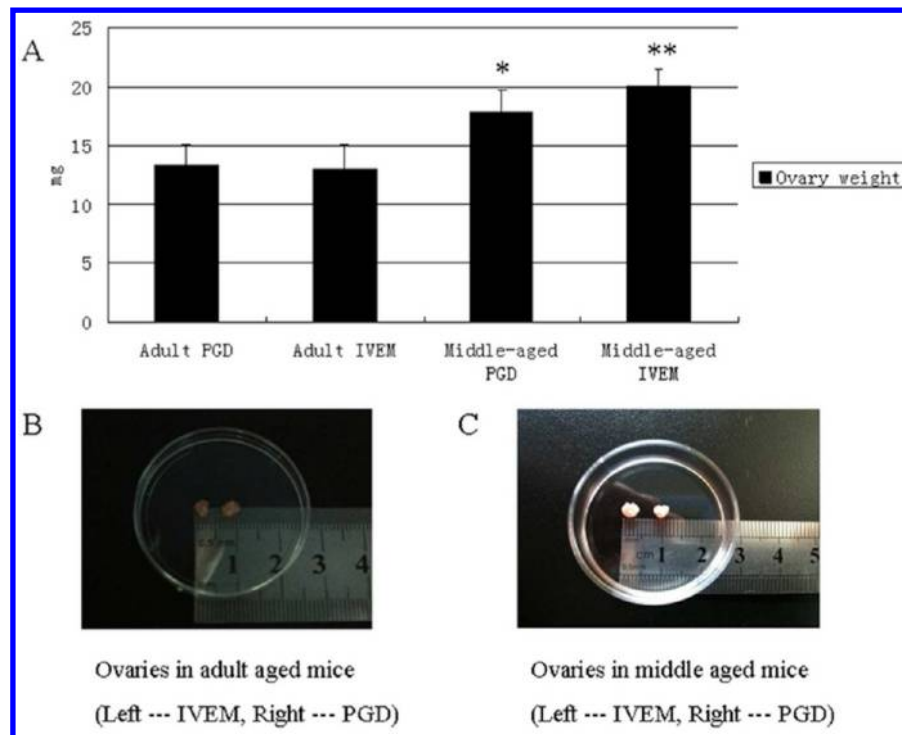
Figure 2. Ovarian morphology in female mice in the biopsied and nonbiopsied groups at different ages. (A) Ovarian weights of female mice in each group. * and ** indicate significant differences, P < 0.05. (B) Ovarian morphology collected from puberty mice. The left image is from a nonbiopsied female, and the right image is from a biopsied female. (C) Ovarian morphology collected from middle-aged mice. The left image is from a nonbiopsied female, and the right image is from a biopsied female.
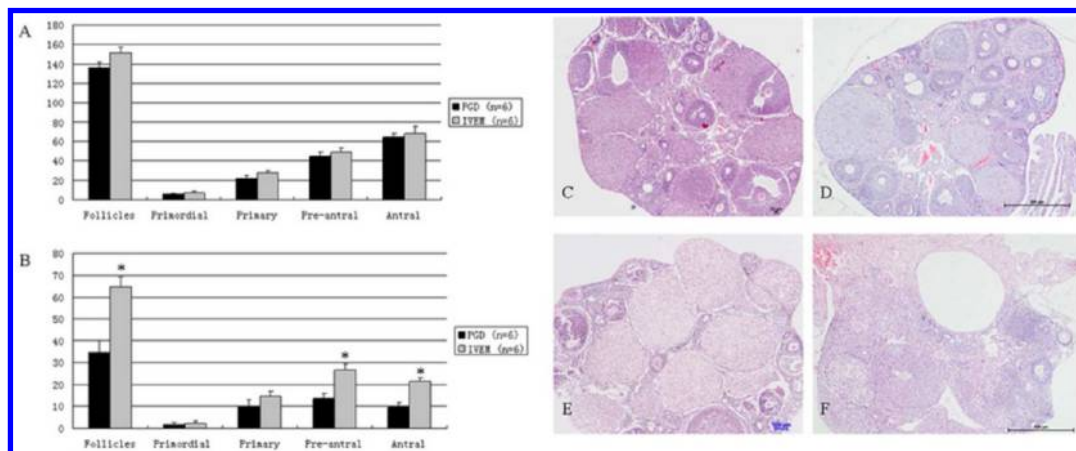

Figure 3. Number and distribution of follicles in the ovaries of mice in the biopsied and nonbiopsied groups at different ages. (A) Number of follicles in different stages in the mouse ovarian tissue in puberty biopsied and nonbiopsied groups. (B) Number of follicles in different stages in the mouse ovarian tissues in middle-aged biopsied and nonbiopsied groups. * indicates significant differences, P < 0.05. (C) Follicle distribution in the ovaries of puberty female in the nonbiopsied group. (D) Follicle distribution in the ovaries of puberty female in the biopsied group. (E) Follicle distribution in the ovaries of middle-aged females in the nonbiopsied group. (F) Follicle distribution in the ovaries of middle-aged females in the biopsied group. The black arrow points to the follicles in different stages.

Table 1. Comparison of Serum Hormone Level Among PGD and IVEM Mice with Different Age[a]

week age	groups	estradiol (pmol/L)	progesterone (nmol/L)	testosterone (nmol/L)	androstenedione (nmol/L)	estrous cycle (days)
10	PGD (n = 18)	142.78 ± 18.85[a]	26.22 ± 1.79[a]	0.67 ± 0.041[a,c]	2.04 ± 0.11[a]	4.29 ± 0.27[a]
	IVEM (n = 15)	148.6 ± 24.23[a]	26.87 ± 2.00[a]	0.58 ± 0.059[a]	2.1 ± 0.17[a]	4.23 ± 0.23[a]
40	PGD (n = 14)	57.07 ± 6.23[b]	5.07 ± 0.87[b]	0.84 ± 0.067[b]	0.77 ± 0.11[b]	6.21 ± 0.33[b]
	IVEM (n = 12)	78.78 ± 5.63[c]	6.25 ± 0.81[b]	0.72 ± 0.066[c]	1.21 ± 0.13[c]	5.32 ± 0.43[c]

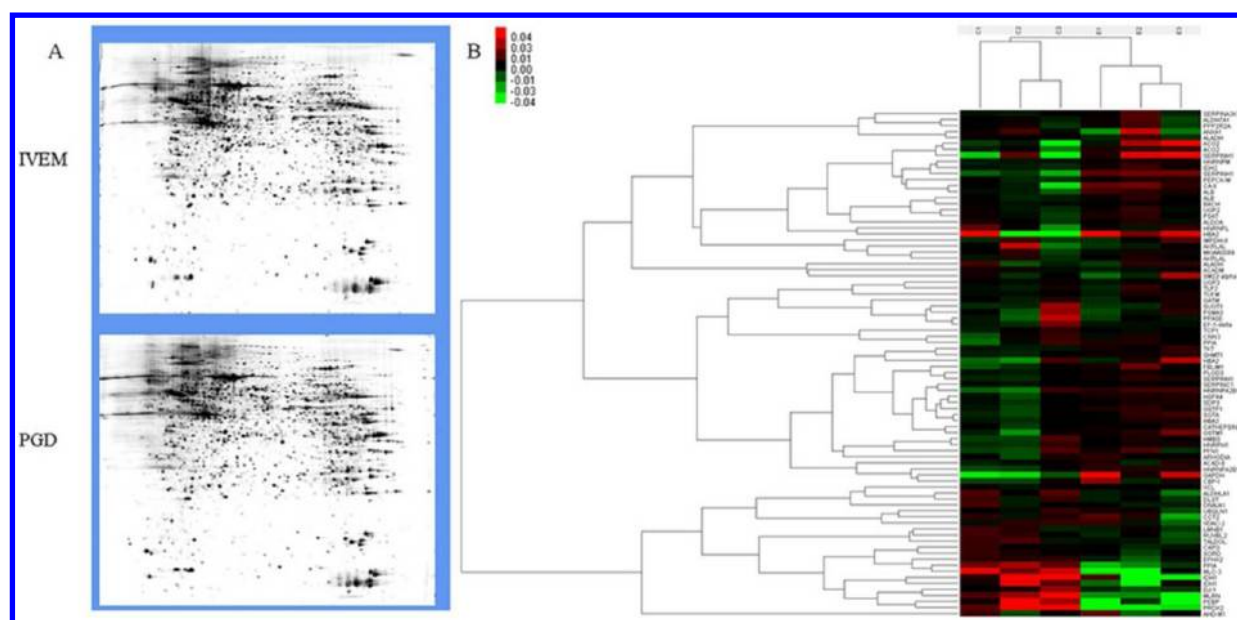[a]Superscripts a−c in the same column mean differ significantly (P < 0.05).

Figure 4. Screening differentially expressed proteins by proteomics method and hierarchical clustering analysis. (A) Photographs of 2-D electrophoresis of puberty female mice in the biopsied and nonbiopsied groups (B) Clustering of brain samples between biopsied and nonbiopsied mice based on 23 differentiated expressed proteins. pH value was determined by 1-D commercial gel, and its range was 3−10 nonlinear. WM range was determined by 2-D gel, its concentration is 12.5%, and its range is 6.5−200 kDa.

Twenty-three differentially expressed spots were detected, of which 10 were significantly up-regulated in the biopsied group, while 13 were down-regulated. Detailed information for the five proteins that were most significantly down- and up-regulated in the biopsied and nonbiopsied groups is listed in Table S2 in the Supporting Information; the detailed information for all differentially expressed proteins is shown in Table S3 in the Supporting Information. The hierarchical cluster diagram demonstrated that protein expression profiles of ovaries from biopsied and nonbiopsied mice are distinctly different (Figure 4B). The possible cellular pathway influenced by embryo biopsy was analyzed with PathwayStudioTM software (version 5.0). The most affected molecular and cellular function was cell apoptosis (eight proteins), cell differentiation (eight proteins), and synthesis (seven proteins; Figure 5).

Four proteins were identified that affected the five cellular pathways (HSPA4, ALDH1A1, VCL, and PSMB8). The cellular pathways affected by these four proteins included all 15 cellular pathways screened by the software. The four proteins underwent Western blotting analysis, and the genes corresponding to the proteins were identified by RT-PCR results to verify the 2-DE results. As shown in Figure 6, the levels of PSMB8 and HSPA4 were significantly increased ($P < 0.05$), and ALDH1A1 was significantly decreased ($P < 0.05$), but VCL was not different in ovarian tissues in biopsied group compared with the nonbiopsied group ($P > 0.05$). The RT-PCR results also showed similar expression profiling of HSPA4, PSMB8, and ALDH1A1, but VCL expression was still not significantly different compared with the nonbiopsied group ($P > 0.05$). The results of ALDH1A1, PSMB8, and HSPA4 were consistent with the results obtained using the ImageMasterTM 2D Platinum Software, but the results of VCL were not in agreement with the proteomics screening results. The four proteins were also identified in the ovarian tissues of middle-aged mice in the biopsied and nonbiopsied groups and showed similar expression profiling (Supplementary Figure 2 in the Supporting Information).

The three differentially expressed proteins (HSPA4, ALDH1A1, and PSMB8) were stained to ascertain protein location in the ovarian tissues by immunohistochemical method. The ALDH1A1 protein was expressed in the cytoplasm of ovarian interstitial and theca cells. The PSMB8 protein was mainly expressed in the cytoplasm and nuclei of cumulus and granular cells around the antral cavity. The HSPA4 protein was expressed in the cytoplasm of cumulus cells and oocytes, and the level of expression in the cumulus cells around the antral follicles was increased. The intensity of expression of these proteins and the distribution of the cells that positively expressed these three proteins were not significantly different, but in middle-aged biopsied ovarian tissues, the distribution of cumulus cells was loose and irregular (Figure 7).

■ DISCUSSION

PGD technology has been applied worldwide since 1990,[2] and more couples have benefitted from this technology because genetic mutations or chromosome aneuploidies were identified before embryo transfer. The high risk of neuronal degenerative diseases has been suggested in a previous study using PGD-biopsied mouse models,[17] and the effects of ICSI technology on male fertility have also been studied;[18,19] however, it is still unclear whether the PGD biopsy procedure has effects on female fertility. Therefore, the present study focused on ovarian tissue differences between biopsied and nonbiopsied mouse models and the significance for risk evaluation of PGD biopsies.

The results of the present study indicated that fertility was not affected by the biopsy procedure in the puberty biopsied group, but the number of follicles in different stages, ovarian weight, the fertility assay, and the levels of estradiol, testosterone, and androstenedione were all decreased in the middle-aged biopsied group. Furthermore, the 3 of the 23 differentially expressed proteins were identified using the proteomics method in puberty biopsied mouse models as well as the differentially expressed proteins in the middle-aged biopsied mouse model. These 3 proteins were related to 12 cellular pathways, including cell apoptosis, cell differentiation, and RNA processing.
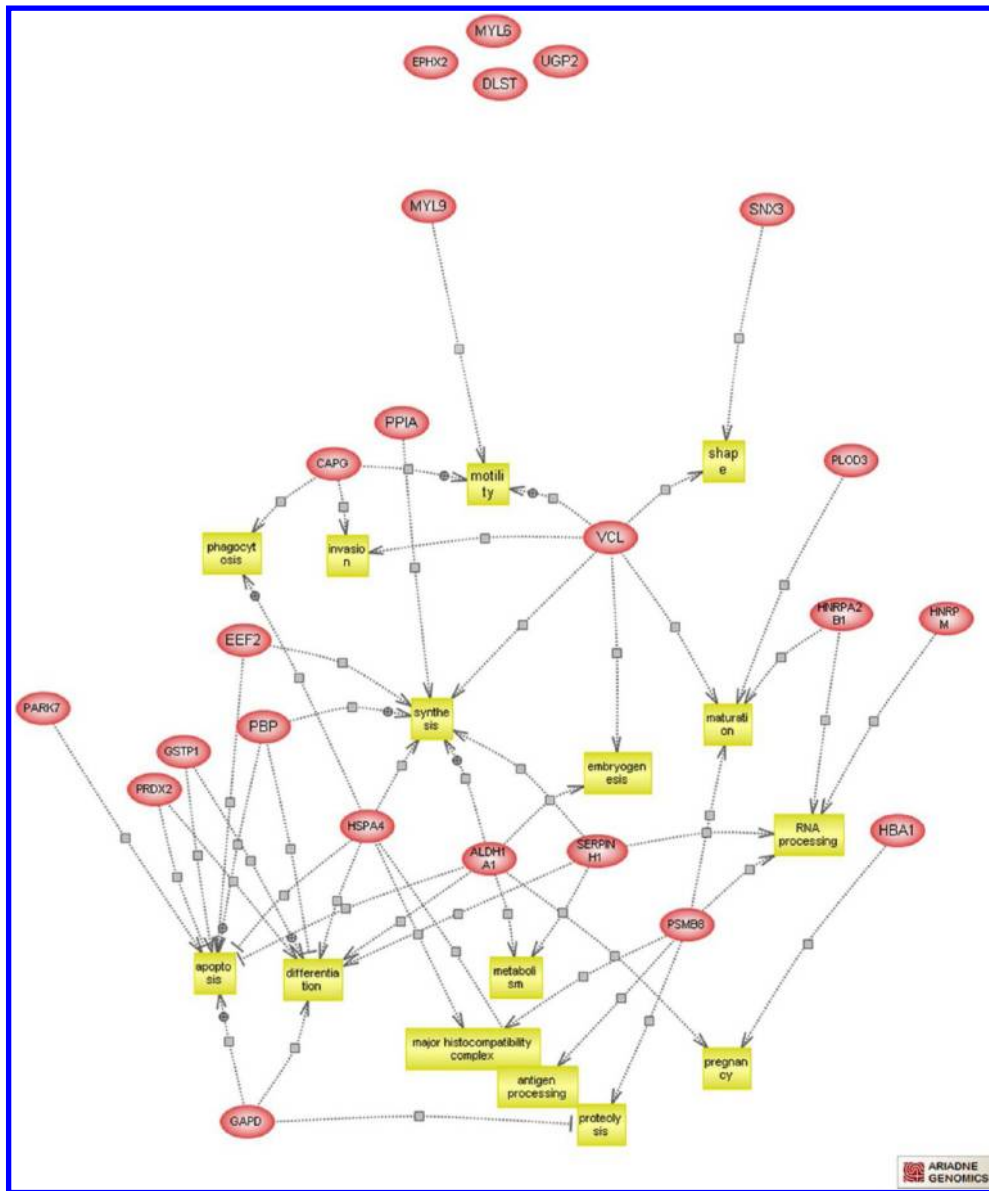
Figure 5. Analysis of cellular pathway affected by these differentiated expressed proteins.
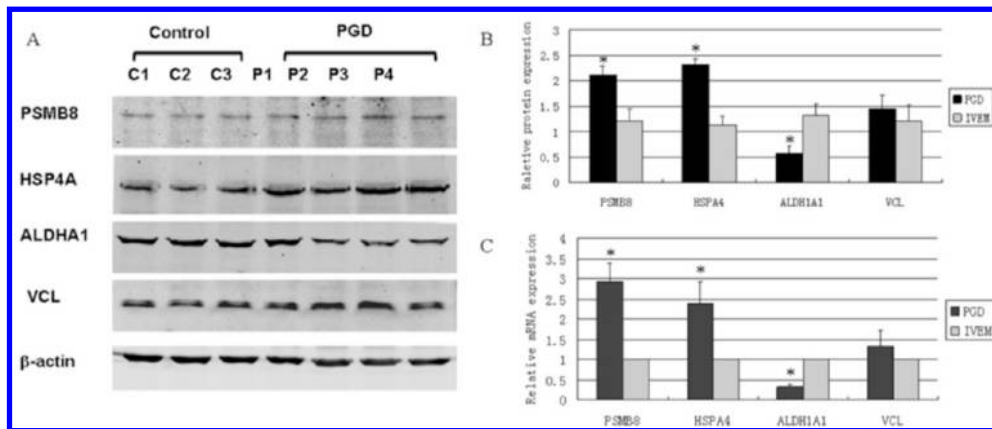

Figure 6. Verification of the differentially expressed proteins and the corresponding genes in the ovaries of puberty mice in the biopsied and nonbiopsied groups. (A) Western blot analyses of each protein are shown. (B) Relative expression of the PSMB8, HSPA4, ALDH1A1, and VCL proteins on the gels. (C) Relative expression of the PSMB8, HSPA4, ALDH1A1, and VCL genes. Error bars represent the standard error of the mean. * indicates significant differences, $P < 0.05$.
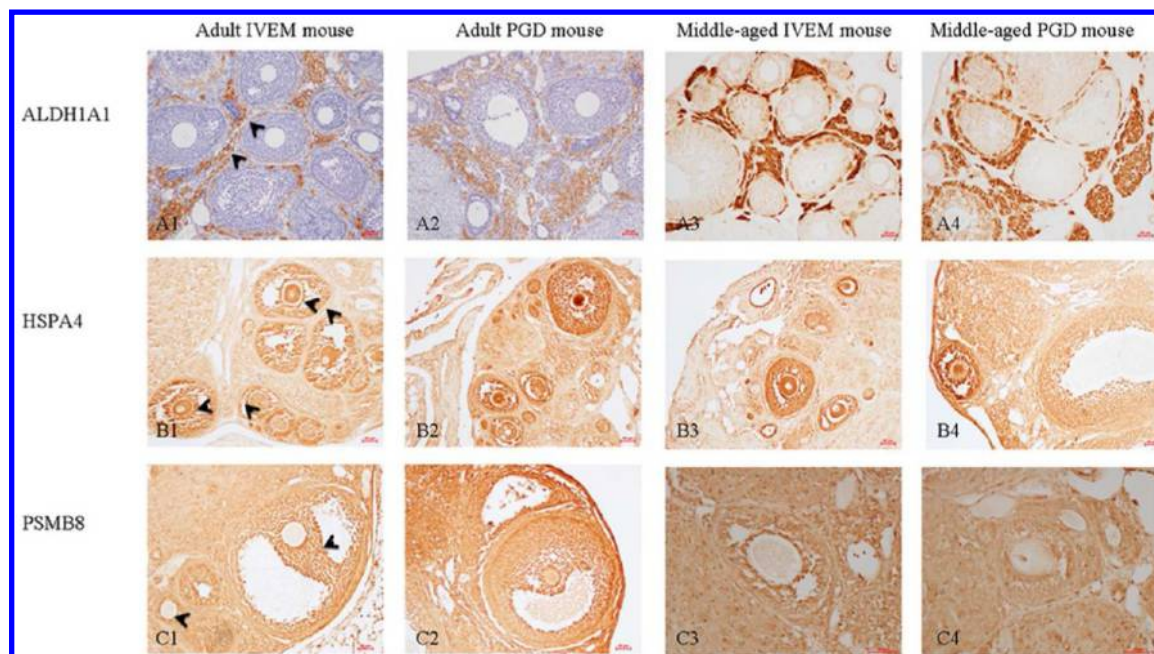
Figure 7. Immunohistochemistry analysis of ALDH1A1, HSPA4, and PSMB8 proteins in the ovarian tissues of puberty and middle-aged mice in the nonbiopsied and biopsied groups. The ALDH1A1 protein was expressed in the cytoplasm of ovarian interstitial and theca cells. The PSMB8 protein was expressed mainly in the cytoplasm and nuclei of cumulus and granular cells around the antral cavity. The HSPA4 protein was expressed in the cytoplasm of cumulus cells and oocytes, and the level of expression in the cumulus cells around the antral follicles was increased. The black arrow points to the location of the proteins.

The fertility in the puberty biopsied group was not different compared with the puberty nonbiopsied group, which was in agreement with a previous study;[17] however, the fertility was decreased in the middle-aged biopsied group compared with the nonbiopsied group, which was possibly attributed to a reduction in ovarian weight and the number of follicles in different developmental stages. The ovarian weight was not normally changed in the mice of the same age unless the mice became pregnant. Jons et al. indicated that ovarian weight, as an index of fecundity, maturity, and spawning periodicity,[27] was also proved by other studies in mice.[28,29] On the basis of our results, the decreased ovarian weight in middle-aged biopsied mice suggested a reduction in ovarian function. In human and other mammals, the ovaries exhibit age-related dysfunction relatively early in life and result in a decrease in the number of follicles.[30] In middle-aged humans, there is usually an acceleration of follicular loss at 35−40 years of age, which results in a decrease in fertility.[31] In the current study, the number of follicles in both middle-aged groups was significantly lower than that in both puberty groups, but more follicles were degenerated in the middle-aged biopsied groups, and thus more severe follicle loss occurred in the biopsied mice models. In humans, the rapid follicle loss at middle age suggests possible premature ovary failure (POF), that is, the loss of ovarian function before 40 years of age.[32]

As the most important organ that is in charge of hormone secretion and endocrine regulation for females, the ovary reveals a marked cycle of ovum and hormone production in the mouse. In the present study, the estrous cycles in the mice from the middle-aged biopsied group were significantly prolonged compared with the nonbiopsied group, which suggested that the hormone levels were possibly influenced in the biopsied group by aging. The hormone testing results also indicated that the levels of estradiol, testosterone, and androstenedione were significantly decreased in the biopsied group. The decrease in estradiol and testosterone could be attributed to the reduction in androstenedione because androstenedione acts as an intermediate step in the biochemical pathway that produces testosterone and estradiol. On the basis of the clinical diagnosis, an abnormal level of androstenedione is often related to unhealthy ovarian function. The increasing androstenedione level in girls or women at risk for polycystic ovarian syndrome (PCOS) is one of the most common female endocrine disorders,[33] and the decrease in the androstenedione level plays a key role in POF, which consists of a decrease in the number of follicles.[34,35] More importantly, Hagemeyer et al. reported that androstenedione, as well as estradiol, impacts neuronal tissues and prenatal neuronal differentiation.[36] In our previous study, we indicated a high risk of neuronal degenerative disorders in biopsied mouse models.[17] Thus, the decrease in the androstenedione level in the middle-aged group possibly has a relationship to the potential neuronal degenerative disorders.

Twenty-three proteins were identified using the proteomics method, which was expressed differently in comparison with the ovaries from the biopsied and nonbiopsied groups, and 15 cellular pathways were affected by these differentially expressed proteins using a bioinformatics method. Four proteins were screened because each of them was related to at least five cellular pathways. After identification by RT-PCR and Western blotting, three proteins, including ALDH1A1, PSMB8, and HSPA4, were selected for further analysis.

Aldehyde dehydrogenase 1 family, member A1, also known as ALDH1A1, is an enzyme that is encoded by the *ALDH1A1* gene in humans.[37] ALDH1A1, 2, and 3 in the fetal ovary and testis have been shown to have key roles in regulating the onset of meiosis in the human fetal ovary by the retinoic acid (RA) signaling pathway.[38] Le Bouffant et al. reported that the beginning of meiosis is often accompanied by an increase in the mRNA level of ALDH1A1, and the meiotic cells disappear when the expression

of ALDH1A1 is inhibited, which was attributed to RA signaling pathway inactivation.[39] This inhibition of meiosis with the down-regulation of ALDH1A1 expression is in agreement with our findings for the decreased fertility and number of follicles. Moreover it has been shown that ALDH1A1 acts as one of the key factors in ovarian autoimmunity associated with unexplained infertility and POF.[40] Furthermore, ALDH1A1 has been identified as a tumor antigen and related to ovarian cancer. ALDH1A1 is also found in cancer stem cells.[41−43]

Heat shock 70 kDa protein 4 (HSPA4) is encoded by this gene and originally suggested to be a member of the heat shock protein 70 family in humans.[44] In a mouse study, HSPA4 was suggested to have important functions in regulating germ cell development, especially for male mice. HSPA4 knockout will result in a significant decrease in fertility in male mice but does not affect female fertility, although the litter size was also decreased slightly.[45,46] In fact, HSPA4 expression is highly enriched in male and female germ cells of prenatal gonads, which indicates its important role in early germ cell development. It is well known that there are waves of germ cell death across most stages of fetal ovarian development, and ∼20% of oocytes in weeks 18−20 of the fetal ovary undergo programmed cell death.[47] In the present study, the differentially expressed protein, HSPA4, was involved in apoptosis regulation, and its abnormal expression would probably influence the apoptosis process of follicle development. Jansen et al. found that a differentially expressed level of the HSP70 family was observed in PCOS patients and suggested that HSP70 is related to follicle development;[48] this result was also confirmed by Salvetti et al.[49]

Proteasome subunit beta type-8 (PSMB8) encodes a catalytic subunit of the immunoproteasome responsible for the generation of peptides presented by major histocompatibility complex (MHC) class-I molecules and is well-known for the Nakajo−Nishimura syndrome that is a kind of autoinflammatory disorder.[50] Although there are no related studies involving the effects of PSMB8 expression on female fertility, some studies have indicated that PSMB8 is a potential diagnostic marker for lipodystrophy syndrome.[51] A mutation in the immunoproteasome subunit, PSMB8, causes autoinflammation and lipodystrophy in humans, which have some relationships to fertility and obstetric complications, especially for obese PCOS patients.[52]

Clinical and basic researchers have gradually paid more attention to the ART safety evaluation at present, and the potential risk has been the subject of human systemic analysis or animal model studies.[53] Because of the different genome and epigenome between mouse and human, it probably produces a deviation of such a risk evaluation. In consideration of the fact of the disclosed ART risks, the evidence provided in the mouse in this work is actually valuable, and this work is typically an example to be used with a large animal as an intermediate model that would better conduct future research close to the humans

In summary, We found that female fertility was decreased in middle-aged mice conceived from the PGD biopsy procedure, which was attributed to the decrease in follicle number and confirmed by anatomic evaluation. Moreover, the results of hormone levels in serum and the estrous cycle were also changed compared with control mice. Three key proteins were identified and screened by the proteomics method, all of which impaired ovarian development or follicle formation directly or indirectly. In addition, each of these three proteins have been found in some tumors or cancers, which indicated that the follow-up should be more careful for female babies conceived from the PGD biopsy procedure when middle-age.

■ ASSOCIATED CONTENT

Ⓢ Supporting Information

Supporting Information Available: This material is available free of charge via the Internet at http://pubs.acs.org.

■ AUTHOR INFORMATION

Corresponding Author

*Tel/Fax: +86-10- 82265080. E-mail: jie.qiao@263.net.

Author Contributions

#Y.Y., Y.Z., and R.L. contributed equally to this work.

Notes

The authors declare no competing financial interest.

■ ACKNOWLEDGMENTS

■ REFERENCES

(1) Steptoe, P. C.; Edwards, R. G. Birth after the reimplantation of a human embryo. *Lancet* **1978**, *2* (8085), 366.

(2) Handyside, A. H.; Kontogianni, E. H.; Hardy, K.; Winston, R. M. Pregnancies from biopsied human preimplantation embryos sexed by Y-specific DNA amplification. *Nature* **1990**, *344* (6268), 768−70.

(3) Gianaroli, L. Preimplantation genetic diagnosis: polar body and embryo biopsy. *Hum. Reprod.* **2000**, *15* (Suppl4), 69−75.

(4) Kokkali, G.; Traeger-Synodinos, J.; Vrettou, C.; Stavrou, D.; Jones, G. M.; Cram, D. S.; Makrakis, E.; Trounson, A. O.; Kanavakis, E.; Pantos, K. Blastocyst biopsy versus cleavage stage biopsy and blastocyst transfer for preimplantation genetic diagnosis of beta-thalassaemia: a pilot study. *Hum. Reprod.* **2007**, *22* (5), 1443−9.

(5) Tarkowski, A. K. Experiments on the development of isolated blastomers of mouse eggs. *Nature* **1959**, *184*, 1286−7.

(6) Moore, N. W.; Adams, C. E.; Rowson, L. E. Developmental potential of single blastomeres of the rabbit egg. *J. Reprod. Fertil.* **1968**, *17* (3), 527−31.

(7) Willadsen, S. M. A method for culture of micromanipulated sheep embryos and its use to produce monozygotic twins. *Nature* **1979**, *277* (5694), 298−300.

(8) Ozil, J. P.; Heyman, Y.; Renard, J. P. Production of monozygotic twins by micromanipulation and cervical transfer in the cow. *Vet. Rec.* **1982**, *110* (6), 126−7.

(9) Tsunoda, Y.; Tokunaga, T.; Sugie, T.; Katsumata, M. Production of monozygotic twins following the transfer of bisected embryos in the goats. *Theriogenology* **1985**, *24* (3), 337−43.

(10) Allen, W. R.; Pashen, R. L. Production of monozygotic (identical) horse twins by embryo micromanipulation. *J. Reprod. Fertil.* **1984**, *71* (2), 607−13.

(11) Chan, A. W.; Dominko, T.; Luetjens, C. M.; Neuber, E.; Martinovich, C.; Hewitson, L.; Simerly, C. R.; Schatten, G. P. Clonal propagation of primate offspring by embryo splitting. *Science* **2000**, *287* (5451), 317−9.

(12) Fleming, T. P.; Pickering, S. J.; Qasim, F.; Maro, B. The generation of cell surface polarity in mouse 8-cell blastomeres: the role of cortical microfilaments analysed using cytochalasin D. *J. Embryol. Exp. Morphol.* **1986**, *95*, 169−91.

(13) Levy, J. B.; Johnson, M. H.; Goodall, H.; Maro, B. The timing of compaction: control of a major developmental transition in mouse early embryogenesis. *J. Embryol. Exp. Morphol.* **1986**, *95*, 213−37.

(14) Shiota, K.; Yamada, S. Assisted reproductive technologies and birth defects. *Congenital Anomalies* **2005**, *45* (2), 39−43.

(15) Hansen, M.; Kurinczuk, J. J.; Bower, C.; Webb, S. The risk of major birth defects after intracytoplasmic sperm injection and in vitro fertilization. *N. Engl. J. Med.* **2002**, *346* (10), 725−30.

(16) Desmyttere, S.; De Rycke, M.; Staessen, C.; Liebaers, I.; De Schrijver, F.; Verpoest, W.; Haentjens, P.; Bonduelle, M. Neonatal follow-up of 995 consecutively born children after embryo biopsy for PGD. *Hum. Reprod.* **2012**, *27* (1), 288−93.

(17) Yu, Y.; Wu, J.; Fan, Y.; Lv, Z.; Guo, X.; Zhao, C.; Zhou, R.; Zhang, Z.; Wang, F.; Xiao, M.; Chen, L.; Zhu, H.; Chen, W.; Lin, M.; Liu, J.; Zhou, Z.; Wang, L.; Huo, R.; Zhou, Q.; Sha, J. Evaluation of blastomere biopsy using a mouse model indicates the potential high risk of neurodegenerative disorders in the offspring. *Mol. Cell. Proteomics* **2009**, *8* (7), 1490−500.

(18) Feng, C.; Wang, L. Q.; Dong, M. Y.; Huang, H. F. Assisted reproductive technology may increase clinical mutation detection in male offspring. *Fertil. Steril.* **2008**, *90* (1), 92−6.

(19) Yu, Y.; Zhao, C.; Lv, Z.; Chen, W.; Tong, M.; Guo, X.; Wang, L.; Liu, J.; Zhou, Z.; Zhu, H.; Zhou, Q.; Sha, J. Microinjection manipulation resulted in the increased apoptosis of spermatocytes in testes from intracytoplasmic sperm injection (ICSI) derived mice. *PLoS One* **2011**, *6* (7), e22172.

(20) Castrillon, D. H.; Miao, L.; Kollipara, R.; Horner, J. W.; DePinho, R. A. Suppression of ovarian follicle activation in mice by the transcription factor Foxo3a. *Science* **2003**, *301* (5630), 215−8.

(21) Liu, J.; Van der Elst, J.; Van den Broecke, R.; Dhont, M. Early massive follicle loss and apoptosis in heterotopically grafted newborn mouse ovaries. *Hum. Reprod.* **2002**, *17* (3), 605−11.

(22) Byers, S. L.; Wiles, M. V.; Dunn, S. L.; Taft, R. A. Mouse estrous cycle identification tool and images. *PLoS One* **2012**, *7* (4), e35538.

(23) Bradford, M. M. A rapid and sensitive method for the quantitation of microgram quantities of protein utilizing the principle of protein-dye binding. *Anal. Biochem.* **1976**, *72*, 248−54.

(24) Wang, L.; Zhu, Y. F.; Guo, X. J.; Huo, R.; Ma, X.; Lin, M.; Zhou, Z. M.; Sha, J. H. A two-dimensional electrophoresis reference map of human ovary. *J. Mol. Med. (Heidelberg, Ger.)* **2005**, *83* (10), 812−21.

(25) Shevchenko, A.; Wilm, M.; Vorm, O.; Mann, M. Mass spectrometric sequencing of proteins silver-stained polyacrylamide gels. *Anal. Chem.* **1996**, *68* (5), 850−8.

(26) Berndt, P.; Hobohm, U.; Langen, H. Reliable automatic protein identification from matrix-assisted laser desorption/ionization mass spectrometric peptide fingerprints. *Electrophoresis* **1999**, *20* (18), 3521−6.

(27) Jons, G. D.; Miranda, L. E. Ovarian weight as an index of fecundity, maturity, and spawning periodicity. *J. Fish Biol.* **1997**, *50* (1), 150−156.

(28) Allan, C. M.; Wang, Y.; Jimenez, M.; Marshan, B.; Spaliviero, J.; Illingworth, P.; Handelsman, D. J. Follicle-stimulating hormone increases primordial follicle reserve in mature female hypogonadal mice. *J. Endocrinol.* **2006**, *188* (3), 549−57.

(29) Williams, S. A.; Stanley, P. Mouse fertility is enhanced by oocyte-specific loss of core 1-derived O-glycans. *FASEB J* **2008**, *22* (7), 2273−84.

(30) Niikura, Y.; Niikura, T.; Tilly, J. L. Aged mouse ovaries possess rare premeiotic germ cells that can generate oocytes following transplantation into a young host environment. *Aging (N. Y.)* **2009**, *1* (12), 971−8.

(31) Menken, J.; Trussell, J.; Larsen, U. Age and infertility. *Science* **1986**, *233* (4771), 1389−94.

(32) Coulam, C. B. Premature gonadal failure. *Fertil. Steril.* **1982**, *38* (6), 645−55.

(33) Veldhuis, J. D.; Pincus, S. M.; Garcia-Rudaz, M. C.; Ropelato, M. G.; Escobar, M. E.; Barontini, M. Disruption of the joint synchrony of luteinizing hormone, testosterone, and androstenedione secretion in adolescents with polycystic ovarian syndrome. *J. Clin. Endocrinol. Metab.* **2001**, *86* (1), 72−9.

(34) Doldi, N.; Belvisi, L.; Bassan, M.; Fusi, F. M.; Ferrari, A. Premature ovarian failure: steroid synthesis and autoimmunity. *Gynecol. Endocrinol.* **1998**, *12* (1), 23−8.

(35) Falsetti, L.; Scalchi, S.; Villani, M. T.; Bugari, G. Premature ovarian failure. *Gynecol. Endocrinol.* **1999**, *13* (3), 189−95.

(36) Hagemeyer, C. E.; Rosenbrock, H.; Singec, I.; Knoth, R.; Volk, B. Different testosterone metabolism by immortalized embryonic and postnatal hippocampal neurons from C57BL/6 mice: a crucial role for androstenedione. *J. Neurosci. Res.* **2000**, *60* (1), 106−15.

(37) Hsu, L. C.; Tani, K.; Fujiyoshi, T.; Kurachi, K.; Yoshida, A. Cloning of cDNAs for human aldehyde dehydrogenases 1 and 2. *Proc. Natl. Acad. Sci. U. S. A.* **1985**, *82* (11), 3771−5.

(38) Childs, A. J.; Cowan, G.; Kinnell, H. L.; Anderson, R. A.; Saunders, P. T. Retinoic Acid signalling and the control of meiotic entry in the human fetal gonad. *PLoS One* **2011**, *6* (6), e20249.

(39) Le Bouffant, R.; Guerquin, M. J.; Duquenne, C.; Frydman, N.; Coffigny, H.; Rouiller-Fabre, V.; Frydman, R.; Habert, R.; Livera, G. Meiosis initiation in the human ovary requires intrinsic retinoic acid synthesis. *Hum. Reprod.* **2010**, *25* (10), 2579−90.

(40) Edassery, S. L.; Shatavi, S. V.; Kunkel, J. P.; Hauer, C.; Brucker, C.; Penumatsa, K.; Yu, Y.; Dias, J. A.; Luborsky, J. L. Autoantigens in ovarian autoimmunity associated with unexplained infertility and premature ovarian failure. *Fertil. Steril.* **2010**, *94* (7), 2636−41.

(41) Penumatsa, K.; Edassery, S. L.; Barua, A.; Bradaric, M. J.; Luborsky, J. L. Differential expression of aldehyde dehydrogenase 1a1 (ALDH1) in normal ovary and serous ovarian tumors. *J. Ovarian Res.* **2010**, *3*, 28.

(42) Landen, C. N., Jr.; Goodman, B.; Katre, A. A.; Steg, A. D.; Nick, A. M.; Stone, R. L.; Miller, L. D.; Mejia, P. V.; Jennings, N. B.; Gershenson, D. M.; Bast, R. C., Jr.; Coleman, R. L.; Lopez-Berestein, G.; Sood, A. K. Targeting aldehyde dehydrogenase cancer stem cells in ovarian cancer. *Mol. Cancer Ther.* **2010**, *9* (12), 3186−99.

(43) Hong, M.; Abastado, J. P. How to develop better screens for anti-cancer therapies? *Oncoimmunology* **2012**, *1* (3), 383−384.

(44) Fathallah, D. M.; Cherif, D.; Dellagi, K.; Arnaout, M. A. Molecular cloning of a novel human hsp70 from a B cell line and its assignment to chromosome 5. *J. Immunol.* **1993**, *151* (2), 810−3.

(45) Held, T.; Barakat, A. Z.; Mohamed, B. A.; Paprotta, I.; Meinhardt, A.; Engel, W.; Adham, I. M. Heat-shock protein HSPA4 is required for progression of spermatogenesis. *Reproduction* **2011**, *142* (1), 133−44.

(46) Held, T.; Paprotta, I.; Khulan, J.; Hemmerlein, B.; Binder, L.; Wolf, S.; Schubert, S.; Meinhardt, A.; Engel, W.; Adham, I. M. Hspa4l-deficient mice display increased incidence of male infertility and hydronephrosis development. *Mol. Cell. Biol.* **2006**, *26* (21), 8099−108.

(47) Albamonte, M. S.; Willis, M. A.; Albamonte, M. I.; Jensen, F.; Espinosa, M. B.; Vitullo, A. D. The developing human ovary: immunohistochemical analysis of germ-cell-specific VASA protein, BCL-2/BAX expression balance and apoptosis. *Hum. Reprod.* **2008**, *23* (8), 1895−901.

(48) Jansen, E.; Laven, J. S.; Dommerholt, H. B.; Polman, J.; van Rijt, C.; van den Hurk, C.; Westland, J.; Mosselman, S.; Fauser, B. C. Abnormal gene expression profiles in human ovaries from polycystic ovary syndrome patients. *Mol. Endocrinol.* **2004**, *18* (12), 3050−63.

(49) Salvetti, N. R.; Baravalle, C.; Mira, G. A.; Gimeno, E. J.; Dallard, B. E.; Rey, F.; Ortega, H. H. Heat shock protein 70 and sex steroid receptors in the follicular structures of induced ovarian cysts. *Reprod. Domest. Anim.* **2009**, *44* (5), 805−14.

(50) Arima, K.; Kinoshita, A.; Mishima, H.; Kanazawa, N.; Kaneko, T.; Mizushima, T.; Ichinose, K.; Nakamura, H.; Tsujino, A.; Kawakami, A.; Matsunaka, M.; Kasagi, S.; Kawano, S.; Kumagai, S.; Ohmura, K.; Mimori, T.; Hirano, M.; Ueno, S.; Tanaka, K.; Tanaka, M.; Toyoshima, I.; Sugino, H.; Yamakawa, A.; Niikawa, N.; Furukawa, F.; Murata, S.; Eguchi, K.; Ida, H.; Yoshiura, K. Proteasome assembly defect due to a proteasome subunit beta type 8 (PSMB8) mutation causes the autoinflammatory disorder, Nakajo-Nishimura syndrome. *Proc. Natl. Acad. Sci. U. S. A.* **2011**, *108* (36), 14914−9.

(51) Agarwal, A. K.; Xing, C.; DeMartino, G. N.; Mizrachi, D.; Hernandez, M. D.; Sousa, A. B.; Martinez de Villarreal, L.; dos Santos, H. G.; Garg, A. PSMB8 encoding the beta5i proteasome subunit is mutated in joint contractures, muscle atrophy, microcytic anemia, and panniculitis-induced lipodystrophy syndrome. *Am. J. Hum. Genet.* **2010**, *87* (6), 866−72.

(52) Vantyghem, M. C.; Vincent-Desplanques, D.; Defrance-Faivre, F.; Capeau, J.; Fermon, C.; Valat, A. S.; Lascols, O.; Hecart, A. C.; Pigny, P.; Delemer, B.; Vigouroux, C.; Wemeau, J. L. Fertility and obstetrical complications in women with LMNA-related familial partial lipodystrophy. *J. Clin. Endocrinol. Metab.* **2008**, *93* (6), 2223–9.

(53) Davies, M. J.; Moore, V. M.; Willson, K. J.; Van Essen, P.; Priest, K.; Scott, H.; Haan, E. A.; Chan, A. Reproductive technologies and the risk of birth defects. *N. Engl. J. Med.* **2012**, *366* (19), 1803–13.